Obtaining, Characterization and Using of Metallosilicate Beads for the Adsorption of Direct Red 95 Dye

EMIL IOAN MURESAN[1]*, NICANOR CIMPOESU[2], ANGELA CEREMPEI[3], DANIEL TIMPU[4] , IOAN GABRIEL SANDU[2,5]*

[1]Gheorghe Asachi Technical University, Faculty of Chemical Engineering and Environmental Protection, 73 Mangeron Blvd., 700050, Iasi, Romania

[2]Gheorghe Asachi Technical University, Faculty of Materials Science and Engineering, 41 Mangeron Blvd., 700050, Iasi, Romania

[3]Gheorghe Asachi Technical University, Faculty of Textiles, Leather Engineering and Industrial Management, 29 Mangeron Blvd., 700050, Iasi, Romania

[4]Institute of Macromolecular Chemistry "Petru Poni",41A Grigore Ghica Voda Alley, 700487, Iasi, Romania

[5]Romanian Inventors Forum, Sf. P. Movila 3, Str. L11, III/3, 700089, Iasi, Romania

Removal of direct dyes from the textile industry wastewaters is a great economic and environmental challenge. In this study, macrospheres with hierarchical porous structure were used as sorbentsf or removal of Direct Red 95dye. The synthesized materials were characterized by water sorption technique, FTIR spectroscopy, DRX and EDAX analyses. The effects of several parameters such as contact time, amount of adsorbent and pH on the adsorption of dye were investigated. The equilibrium data were evaluated using Langmuir, Freundlich, Temkin and Dubinin-Radushkevish isotherms.The values of correlation coefficients, R^2 showed that the Langmuir model best fitted with the experimental data.The kinetic parameters were calculated using four kinetic models: the pseudo first order model, pseudo second order model, Elovich model and modified Freundlich kinetic model. The pseudo first order model was found to be the most suitable to describe the adsorption kinetics.

Keywords: hierarhical porous beads, XRD, direct dye, adsorption isotherms, kinetic models

Many of the dyes used in the dyeing industries, paper and pulp industries, textile industries, and many other industries may affect the aquatic ecosystem due to their toxicity and persistence after being released into the natural water. From the category of dyes used in the textile industry, the direct dyes are commonly used for dyeing of textile materials from cellulosic fibers, due to the advantages they present (a wide range of colors, low cost, easy application technology), but only about 80% of the dye amount from the dyeing bath is taken over by the material in the dyeing process. The presence of very small amounts of dyes in water (less than 1 ppm for some dyes) is highly visible and undesirable [1]. Among several chemical and physical treatment methods (ultrafiltration, chemical precipitation, oxidation, ion exchange, adsorption), the adsorption process is an attractive alternative way for the removal of dyes from the wastewaters. Numerous studies have been devoted to the study of dyes adsorption mechanism and to the search for a suitable adsorbent [2]. In the literature, commercial activated carbon, clays, modified silica hybrids, zeolites, bentonite and montmorillonite are the most commonly used adsorbents for environmental applications [3-25]**.** In the recent years, mesoporous molecular sieves have been accepted as one of the appropriate adsorbents for the removal of dyes from the wastewater [26, 27]. The sol-gel method has been used for the synthesis of the inorganic macrospheres and the templating technique was widely applied to control the morphology of inorganic materials.

The objectives of this work are: (1) to obtain porous hierarchically metallosilicate beads, (2) to investigate the adsorption capacity of metallosilicate beads in removal of direct red dye from the aqueous solution, (3) to determine the effects of the adsorbant dosage, contact time, initial concentration of the direct dye on the adsorption capacity of the used adsorbent, (4) to study the applicability of various adsorption isotherms, (5) to find the kinetic model that best fits the adsorption data.

Experimental part

Material and Methods

Adsorbate

Commercial direct dye Siriuslichtscharlach BN (C.I. Direct Red 95) was obtained from Dye Star Company and used without any further purification. The structure of dye is shown in figure 1.

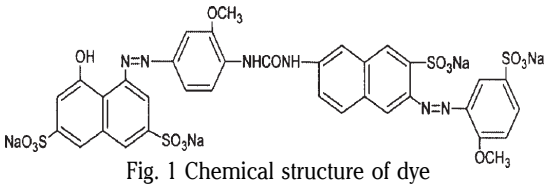

Fig. 1 Chemical structure of dye

Adsorbent synthesis

The synthesis of metallosilicate beads used as adsorbent was performed as follows: 0.96 g gelatin was dissolved in an aqueous solution (containing 1.4 mL HCl 37% and 10.6 mL water) under vigorous stirring until a clear solution was formed. In this solution were introduced 0.5 g $Cr(NO_3)_3$ x $9H_2O$, 0.4439 g $CeCl_3$ x $9H_2O$, 0.1944 g $AlCl_3$ x $6H_2O$ and 0.1095 g $ZnCl_2$. After dissolution of the salts a yeast cells suspension (6 g yeast cells dispersed in 3 mL distilled water were heated at 80°C for 2 h)was added under stirring**.** Subsequently 4 mL TEOS were poured and

* *email: eimuresan@yahoo.co.uk; gisandu@yahoo.com*

the mixture thus prepared was kept under stirring for 6 hours. 12 g of 4% chitosan solution were added over the resulting gel and the stirring continued until the complete homogenization of the mixture.The obtaining gel was finally added dropwise with a syringe pump into a precipitation bath containing an ammonia solution (25% v/v). The beads prepared in this way were kept into ammonia coagulating solution (to harden) for 40 min, separated by filtration in a Buchner funnel and then dried at 50°C for 12 h. The dried samples were calcinated in air at 650°C for 24 h in order to remove the template.

Characterization techniques

The porous structure characteristics of the calcined samples, including surface area, pore volume and and pore diameter were obtained from the conventional analysis of water adsorption–desorption isotherm recorded on an automated gravimetric analyzer IGAsorp produced by Hiden Analytical, Warrington (UK).

The XRD patterns of the samples were recorded on a Philips X PERT MPD diffractometer using a nickel-filtered Cu Kα radiation (λ = 0.15418 nm) derived from a high power rotating anod X-ray generator. The instrument was operated in continuous mode at a generator tension of 40 kV and a generator current of 100 mA. The small angle X-ray diffraction measurements were recorded for a 2θ angle from 0.7° to 10° with a step size of 0.02 and a step time of 2 s.The wide angle X-ray diffraction measurements were performed in the 2 range of 20-80° at a scanning speed of 1°/min. To allow the low angle measurements the 0.1° receiving slit in the diffractometer was replaced by a 0.25° one. The evaluation of the diffractograms was made with the DIFFRAC/AT software.

Scanning electron microscopy with X-ray microanalysis (SEM/EDX) was carried out with Quanta 200 (Fei) scanning electron microscope coupled with an energy dispersive X-ray analyzer. Samples were prepared by dispersing dry powder shell on copper support and coated with gold by cathode deposition using an EMITECHK 550 apparatus

The FTIR spectra were performed with the FTIR spectrometer Vertex 70 (Bruker) using the conventional KBr-disk technique. Before each measurement, the samples were degassed for more than 3h at 473 K and 1.33 Pa. Infrared spectra in the range 4000 - 400 cm^{-1} were obtained by the co-addition of 32 scans with a resolution of 2 cm^{-1}.

Adsorption studies

The metallosilicate beads were tested as *adsorbent* for the dye Direct Red 95. The sorption studies were performed at room temperature by the immersion method. Various parameters such as: mass of adsorbent (25–150 mg), dye concentration and *p*H (2–10) were studied. Each experiment was duplicated under identical conditions. The concentration of the dye in the aqueous solution was determined by using a UV-Vis spectrophotometer at wavelength of 496 nm. Prior to analysis, a calibration curve (y = 0.0088x,R^2 =0.999) has been obtained and the concentrations of dye were determined from the linear calibration curve established. The amount of dye adsorbed per unit mass of adsorbent at equilibrium, q_e (mg/g), was calculated by the following expression:

$$q_e = \frac{(C_0 - C_e) \cdot V}{w} \quad (1)$$

where C_0 and Ce are the initial and respectively the equilibrium dye concentrations in solutions (mg/L), V is the volume of the solution (L) and w is the mass of the adsorbent (g).

The amount of dye adsorbed per unit mass of adsorbent at any time t, q_t (mg/g) was calculated from equation:

$$q_t = \frac{(C_0 - C_t) \cdot V}{w} \quad (2)$$

where C_t (mg/g) is the liquid phase concentration of the dye at any time t.

Results and discussions

Characterization of metallosilicate beads used as adsorbent

Determination of textural properties from the water physisorption data

The BET specific surface area (S_{BET}) and constant (C_{BET} – related exponentially to the enthalpy of adsorption in the first adsorbed layer) were calculated applying the Brunauer Emmet Teller equation to the adsorption branch of the isotherm over the relatively low relative pressure range (p/p_0 = 0.05-0.30). The micropore volume (V_{micro}), the mesopore volume (V_{meso}) the microporous surface area (S_{micro}) and the total surface area (S_t) for the trimodal material were estimated using the modified t-plot method proposed by Mikhail and Hagymassy [28-31].

The total pore volume (V_p), which included all pores (micro, meso and macro), was calculated as difference between the apparent specific volume (V_{ap}) and the specific volume of the solid metallosilicate skeleton (V_r): $V_p = V_{ap} - V_r = 1/\rho_{ap} - 1/\rho_r$ where the apparent density (ρ_{ap}) and the skeletal density (ρ_r) were determined by mercury and respectively helium pycnometry. The macropore volume was calculated by subtracting the volumes of micro and mesopores from the total pore volume. The most important textural properties are summarized in table 1.

Energy dispersive X-ray analysis (EDAX)

The elemental composition of the studied adsorbent was determined by EDAX analysis. The initial composition of the gel used to obtain the metallosilicate beads used in adsorption experiments, expressed as molar ratios Si : Cr : Ce : Al : Zn (input values) and the final composition of the synthesized material (after calcination) calculated from EDAX analysis data (output values) are listed in table 2.

FTIR analysis

FTIR spectrum of the synthesized metallosilicate sample is shown in figure 2.

S_{BET} (m^2/g)	V_{micro} (cm^3/g)	V_{mezo} (cm^3/g)	V_{macro} (cm^3/g)	S_t (m^2/g)	V_t (cm^3/g)
294	0.051	0.055	0.232	289	0.338

Table 1
TEXTURAL PROPERTIES OF THE CALCINED SAMPLE

Table 2
THE VALUES OF SILICON/ METALS MOLAR RATIOS CORRESPONDING TO THE SYNTHESIS GEL (INPUT RATIO) AND RESPECTIVELY TO THE CALCINED ADSORBENT SAMPLE (OUTPUT RATIO)

Metallosilicate composition	Si	Cr	Ce	Al	Zn
Input molar ratio	1	0.07	0.07	0.045	0.045
Output molar ratio	1	0.084	0.084	0.065	0.033

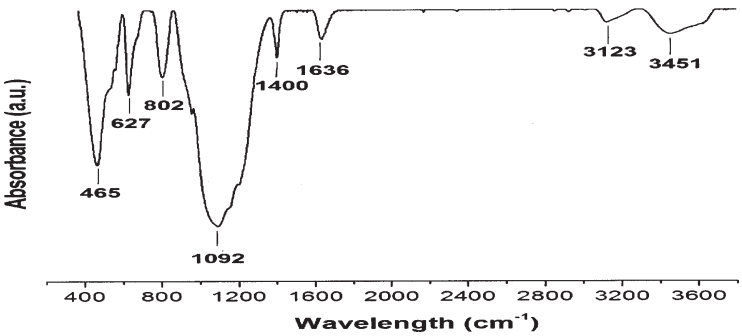

Fig. 2. FTIR spectra of the calcined metallosilicate samples

The peak at 465 cm^{-1} is assigned to overlapping of the bending mode vibrations of Si – O – Si and Si-O-M bonds respectively. The symmetric stretching vibrations of Si–O–Si bonds occur at 802cm^{-1} while the asymmetric stretching vibrations of the Si–O–Si bonds exhibit their peaks at 1092 cm^{-1}. The signal detected at 627 cm^{-1} is assigned to the stretching vibrations of Si-O-Me bonds. The peaks at 1636 $cm^{-1}$are related to the bending mode vibrations of adsorbed water molecules. The peak at 1400 cm^{-1} is attributed to the bending mode vibrations of the C-H bonds from the uncalcined organic phase. The very small peaks at 2855 cm^{-1} and 2926 cm^{-1} are assigned to the stretching vibrations of C-H bonds from the template molecules (that were not removed by calcination). The peak at 3123 cm^{-1} corresponds to the stretching vibrations of defective Si-O groups. The broad band around 3451 cm^{-1} may be attributed to the -OH stretching vibrations of adsorbed water molecules overlapped with the –OH stretching vibrations of the surface silanols.

Small angle X-ray diffraction experiments

Small angle X-ray scattering(SAXS) was used to identify the structural ordering of the material under study. The small-angle X-ray scattering spectra of the calcined sample is shown in figure 3a.

The XRD pattern appears to consist of a single broad diffraction peak centered at the 2θ of 1.535°, which corresponds to a interplanar d-spacing of 5.75 nm calculated from the Bragg equation ($2d \sin\theta = \lambda$, where λ = 1.5406 A° for the Cu Kα line). The broadness of the single peak in the low angle range and the absence of additional higher degree peaks suggest that: (1) the sample presents a short-range ordering derived from the assembly of chitosan and gelatin macromolecules; (2) this sample lacks the long-range ordering in structure.

Wide angle X-ray diffraction experiments

Wide angle X-ray diffraction analysis is the most frequently used technique to characterize the crystallinity and the phase purity of the materials. Figure 3b shows the wide angle XRD pattern of the synthesized metallosilicate material.

The phase identification is usually performed by XRD diagrams using a search match program supported by JCPDS cards. Matching the XRD pattern with the JCPDS data does not allow to unambiguously characterizing the phases present when the sample contains several transition metals due to the systematic peak overlap. Moreover it is difficult to distinguish between (1) the diffraction peaks attributed to various polymorphic forms of a certain material (when they are very closed to each other) and (2) the diffraction peaks of metallic oxides or the corresponding metallosilicates. In table 3 are summarized the values of the peaks from the recorded DRX pattern and the closest peak values (which best match with the observed diffraction peaks) extracted from the JCPDS database.

The high intensities of the peaks located at 2θ = 28.65°; 35.85°; 42.64°; 57.66° and 63.2° are explained by the overlapping of the peaks coming from several oxides. The broad band between 2θ = 15 - 30° is characteristic to the amorphous silica.

Adsorption studies

Effect of adsorbent concentration on dye removal

The results of the experiments carried out with various adsorbent concentrations are presented in figure 4. With the increase in the adsorbent concentration, from 0.05 g to 0.3 g, the percentage of uptaken dye increased. This was attributed to the increase of the number of available adsorption sites.

Effect of the contact time and dye concentration

The adsorption capacity of the dye on metallosilicate beads versus time is illustrated in figure 5. It can be seen that the dye is adsorbed faster in the first hours. Thereafter the adsorbed amount increases slowly with the prolonging of the contact time until the equilibrium was reached at 120 h.

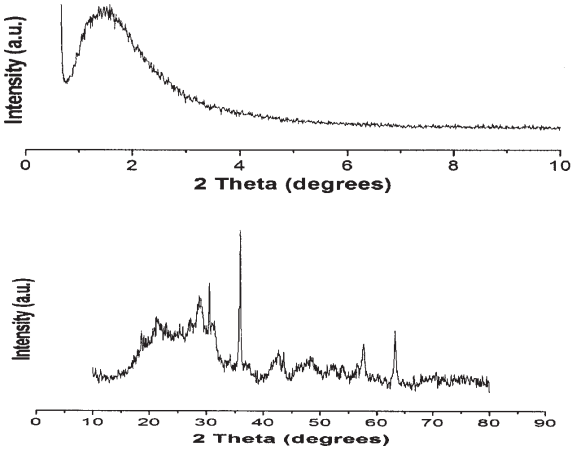

a. Small angle XRD pattern

b. Wide angle XRD pattern

Fig.3. XRD patterns for the calcined metallosilicate sample

Observed (2θ)	Angle JCPDS (2θ)	Oxide	JCPDS card no.	Space group	(hkl) Miller indices
21.18	20.80	SiO_2 quartz	85-0794	$P3_221$	(100)
25.50	25.37	α Al_2O_3	42-1468	R3c	(012)
	24.484	Cr_2O_3	38-1479	R3c	(012)
28.65	28.50	SiO_2	27-1402	$P3_221$	(200)
	28.52	CeO_2	34-0394	Fm3m	(111)
30.44	31.60	SiO_2	27-1402	$P3_221$	(111)
	31.30	CeO_2	34-0394	Fm3m	(200)
	31.72	ZnO	36-1451	$P6_3mc$	(100)
34.11	34.42	ZnO	36-1451	P63mc	(002)
	33.584	Cr_2O_3	38-1479	R3c	(104)
	34.89	α Al_2O_3	42-1468	R3c	(104)
35.83	35.40	α Al_2O_3	42-1468	R3c	(104)
	36.181	Cr_2O_3	38-1479	R3c	(110)
	36.25	ZnO	36-1451	P63mc	(101)
	35.70	CeO_2	34-0394	Fm3m	(104)
42.64	41.463	Cr_2O_3	38-1479	R3c	(113)
	43.04	α Al_2O_3	42-1468	R3c	(113)
48.25	47.53	ZnO	36-1451	P63mc	(102)
	47.40	CeO_2	34-0394	Fm3m	(220)
52.28	52.28	α Al_2O_3	42-1468	R3c	(024)
57.66	57.26	α Al_2O_3	42-1468	R3c	(116)
	56.60	ZnO	5-0664	P63mc	(110)
	56.52	CeO_2	34-0394	Fm3m	(311)
63.20	63.421	Cr_2O_3	38-1479	R3c	(214)
	61.33	α Al_2O_3	42-1468	R3c	(018)
	62.86	ZnO	36-1451	P63mc	(103)
70.57	69.09	ZnO	36-1451	P63mc	(201)
75.52	76.90	α Al_2O_3	42-1468	R3c	(119)

Table 3
COMPARISON BETWEEN THE OBSERVED AND THE STANDARD X-RAY POWDER DIFFRACTION PEAKS OF THE CALCINED METALLOSILICATE SAMPLE

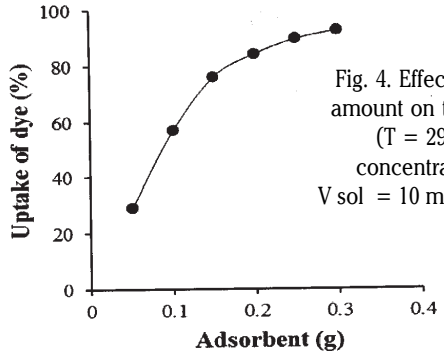

Fig. 4. Effect of the adsorbent amount on the adsorption dye (T = 298 K, initial dye concentration = 20 mg/L, V sol = 10 ml, contact time 96 h)

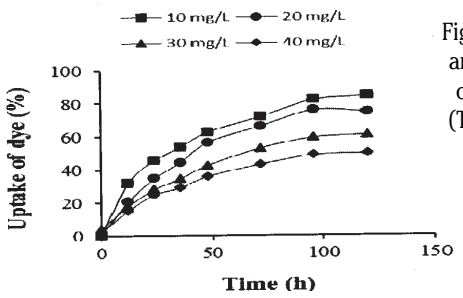

Fig. 5. Effect of the time and dye concentration on the uptake of dye (T = 298 K, adsorbent amount 0.15 g, V sol = 10 mL)

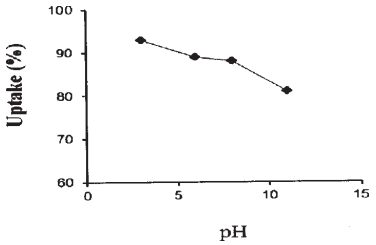

Fig. 6. Effect of *p*H on the adsorption of dye (T = 298 K, initial concentration of dye = 20 mg/L, V sol = 10 mL, contact time 120 h)

From figure 5 one notices that by increasing of the initial dye concentration in solution decreases the amount of dye adsorbed onto metallosilicate beads. This behaviour can be explained by the change of the ratio between the number of the dye molecules and the number of the available adsorption sites. The adsorption process takes place in three steps: (1) the molecules of dye reach to the boundary layer; (2) the molecules diffuse to the surface of adsorbent; (3) the dye molecules diffuse through the porous structure of the adsorbent and finally are adsorbed. The diffusion of direct dye from the bulk solution towards the surface of the metallosilicate adsorbent can be considered as the rate-determining step.

Effect of pH

The adsorption of dye onto the metallosilicate beads is significantly influenced by the change of initial *p*H of the dye solution (fig. 6).

In this study, the effect of solution *p*H on the adsorption of dyes was investigated in the range 2 to 11, while the initial concentration (20 mg/L) and the temperature (25°C) were kept constant. The results indicate that the dye adsorption decreases with the increase of the *p*H solution. Generally, by decreasing of *p*H increases the positive charge on the adsorbent surface and consequently increases the electrostatic attraction between the anionic sulfonic groups of dye and the protonated groups from the surface of adsorbent.

Adsorption Isotherms

Adsorption isotherms describe the relationship between the amount of solute adsorbed onto the solid and the equilibrium concentration of the solute in solution at a given temperature.In order to quantify the affinity of the metallosilicate beads for the direct dye, four widely used isotherm models (Langmuir, Freundlich, Tempkin and Dubinin-Radushkevish) were used to analyze the data obtained from the adsorption process.

Langmuir isotherm

The Langmuir equation which is applicable to homogeneous adsorption systems is based on the assumption that only a monolayer of dye can cover the surface of the adsorbent (each site can hold at most one

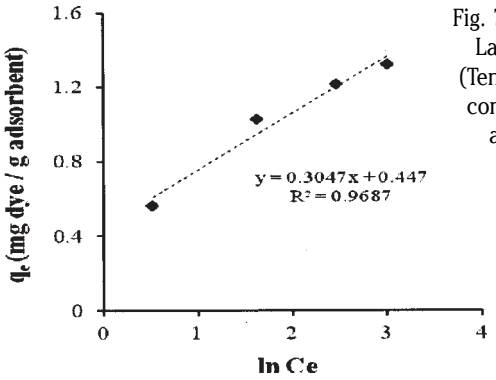

Fig. 7. Linear plot of the Langmuir isotherm (Temperature = 298 K, contact time = 120 h, adsorbent dose 0.15 g/ 10 mL)

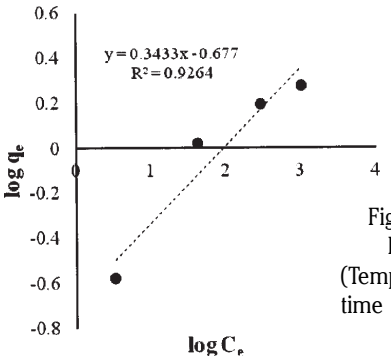

Fig. 8. Linear plot of the Freundlich isotherm (Temperature = 298 K, contact time = 120 h, adsorbent dose 0.15 g/ 10 mL)

molecule, all the adsorption sites are equivalent and there are no interactions between the adsorbate molecules on adjacent sites).

The linear form of the Langmuir equation may be written as equation:

$$\frac{C_e}{q_e} = \frac{1}{q_m} \cdot C_e + \frac{1}{K_a \cdot q_m} \quad (3)$$

where q_e (mg/g) is the amount of dye adsorbed per unit weight of adsorbent, Ce (mg/L) is the equilibrium concentration of the dye in the bulk solution, q_m (mg/g) is the maximum amount of adsorbate per unit weight of adsorbent required to form a complete monolayer on the surface and K_a(L/mg) is the Langmuir isotherm constant related to the affinity of the adsorption sites.

The plot of Ce/qe versus Ce gives a straight line of slope $1/q_m$ and intercept $1/Ka \cdot q_m$ (fig. 7). The validity of the Langmuir adsorption process is assessed by a dimensionless constant separation factor R_L, as equation :

$$R_L = \frac{1}{1 + K_a \cdot C_0} \quad (4)$$

where C_0 is the initial concentration of dye (mg/ L).

The value of R_L indicates whether the isotherm is irreversible ($R_L = 0$), favorable ($0 < R_L < 1$), linear ($R_L = 1$) or unfavorable ($R_L > 1$). The R_L values calculated are found to lie between 0.217 and 0.065 for the initial concentration values in the range 10 – 40 mg/L. The obtained R_L values show that the adsorption of dye on metallosilicate beads is favorable irrespective of the initial concentration.

Freundlich isotherm

The Freundlich expression is an empirical model employed to describe the heterogeneous systems (assumes a heterogeneous energetic distribution of the active sites on the adsorbate surface and takes into account the interactions between the adsorbed molecules). This model is not restricted to the formation of the monolayer. The linear form of the Freundlich isotherm is represented by the equation:

$$\log q_e = \log K_F + \frac{1}{n} \log Ce \quad (5)$$

where q_e(mg/g)is the amount of dye adsorbed per unit weight of the sorbent, C_e (mg/L)is the equilibrium concentration of the dye in the bulk solution, K_F(mg/g) is a measure of the adsorption capacity and 1/n corresponds to the adsorption intensity (the higher the 1/n value, the more favorable is the adsorption).

The values of Freundlich constants 1/n and $K_F$were calculated from the slope and the intercept of the linear plot of log $q_e$versus log C_e (fig. 8 and table 4). The constant K_F is an approximate indicator of the adsorption capacity, while 1/n is a function of the strength of adsorption. The value of n describes the adsorption characteristics as follows: n = 1, there is no interaction between the adsorbed species which means a homogenous adsorption; n > 1, favorable adsorption; n < 1, unfavorable adsorption. A value of n greater than unity assumes a heterogeneous surface with minimum interaction between the adsorbed atoms.

Temkin isotherm

This isotherm explicitly takes into the account the adsorbent–adsorbate interactions and suggests that because of these interactions the energy of adsorption is a linear function of the surface coverage. The Temkin isotherm is usually valid only for intermediate ion concentrations. By ignoring the extremely low and large values of concentrations, the model assumes that due to these interactions the heat of adsorption (function of temperature) of all molecules in the layer would decrease linearly with surface coverage. The linear form of the model is given by the following equation:

$$q_e = \frac{R \cdot T}{b_T} \cdot \ln K_T + \frac{R \cdot T}{b_T} \ln C_e \quad (6)$$

where R is the gas constant, T is the absolute temperature (K), $1/b_T$ is the Temkin constant related to the heat of adsorption (kJ/mol) which indicates the adsorption intensity of the adsorbent and K_T (L/g) is the Tempkin constant related to the adsorption capacity.

The Temkin adsorption constants were determined from the slope and intercept obtained by the linear plotting of the quantity of adsorbed dye q_e against ln C_e,(fig. 9 and table 4).

Dubinin-Radushkevish isotherm (D-R)

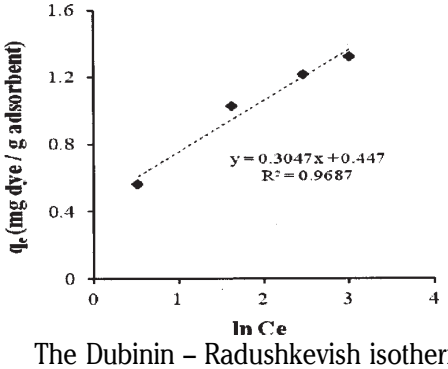

Fig. 9. Linear plot of the Tempkin isotherm (Temperature = 298 K, contact time = 120 h, adsorbent dose 0.15 g/ 10 mL

The Dubinin – Radushkevish isotherm (D-R) model is more general than the Langmuir isotherm since it does not assume a homogenous surface or constant sorption potential. This model is often used to determine the type of sorption (physical or chemical). The D-R equation is:

$$\ln q_e = \ln q_m - B_D \cdot \varepsilon^2 \quad (7)$$

where: q_e is the amount of dye adsorbed per unit weight of adsorbent (mg/g), q_m is the D-R constant representing the theoretical monolayer saturation capacity (mg/g) and B_D (mol^2 / J^2) is a constant related to the mean free energy of adsorption per mol of the adsorbate and ε is the Polanyi potential which is given by equation:

$$\varepsilon = R \cdot T \cdot \ln(1 + 1/C_e) \quad (8)$$

where T is the temperature of solution (K) and R is the gas constant and is equal to 8.314 J/mol x K. Ce is the equilibrium concentration mg/L. The value of the sorption energy (apparent energy of adsorption) E can be calculated from D–R parameter B_D as follows:

$$E = 1/\sqrt{2 \cdot B_D} \quad (9)$$

The linear plot of ln q_e against ε^2 at 298 K is shown in figure 10.

The constants q_m and B_D were calculated from the intercept and respectively the slope of the straight line. The values of D-R isotherm parameters and the regression parameter R_c are given in table 4. If the value of E lies between 8 - 16 kJ/mol the sorption process is a chemisorption one, while the values lower than 8 kJ/ mol indicates a physical adsorption.

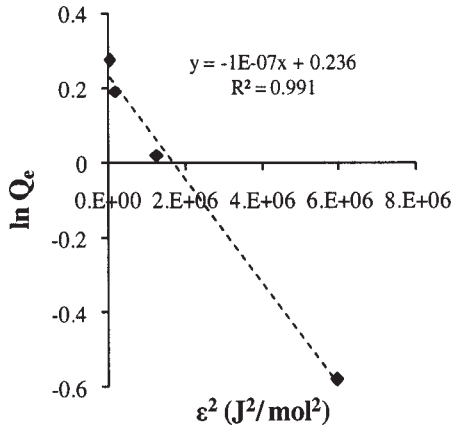

Fig. 10. Linear plot of the Dubinin-Radushkevish isotherm (Temperature = 298 K, contact time = 120 h, adsorbent dose 0.15 g/ 10 mL)

The value obtained for the apparent energy of adsorption E = 2.236 kJ/mol, indicated physical adsorption between the adsorbent and the direct dye molecules.

Comparing the quality of fitting for the four models of isotherms in terms of correlation coefficient values, R_c (shown in figures 7-10), it can be seen that the Langmuir isotherm shows the best agreement with the experimental data, followed by the Dubinin-Radushkevishi and respectively Temkin isotherm, while the least fit was obtained with the Freundlich isotherm.The well fit of experimental data to the Langmuir isotherm indicates that the monolayer adsorption is dominant.

Adsorption kinetics

Study of adsorption kinetics is important because the rate of adsorption (which is one of the criteria for the efficiency of adsorbent) and also the mechanism of adsorption can be concluded from the kinetic studies.The knowledge of adsorption kinetic parameters is required to select the optimal operational condition for treatment of wastewaters and to design the full scale processes. The kinetics of adsorption of direct Red 95 dye was examined using several kinetic models: the pseudo first order model, pseudo second order model, Elovich model and modified Freundlich kinetic model. The sorption behaviour of the dye was analyzed using linear regression.

Pseudo first order model (Lagergren)

This model is commonly used for homogeneous sorbents and physical sorption. This model supposes that the rate of adsorption is influenced by the adsorbate concentration (the sorption rate is proportional to the dye concentration) and by the number of free sites for adsorption. The experimental results are expressed using the following kinetic equation:

$$\ln(q_e - q_t) = \ln q_e - k_1 \cdot t \quad (10)$$

where q_e and q_t are the amounts of adsorbed dye per unit mass of adsorbent (mg/g) at the equilibrium and respectively at time t (h), and $k_1(h^{-1})$ is the pseudo-first order kinetic constant [26].

The values of k_1 and q_e are determined from the slope and respectively the intercept of the straight line obtained when plotting $\ln(q_e - q_t)$ versus time t (fig. 11a). The obtained values of k_1, q_e and R^2 (coefficient of correlation) are presented in table 5.

Pseudo-second order model

The pseudo second order model, proposed by Ho McKay and Yeung [20], is based on the assumption that the rate-limiting step may be chemisorption involving valence forces through the sharing or exchange of electrons between adsorbent and adsorbate.

The linear form of this model can be represented by the following equation:

$$\frac{1}{q_e - q_t} = \frac{1}{q_e} + k_2 \cdot t \quad (11)$$

where: q_t and q_e are the amounts adsorbed at time t and at equilibrium respectively (mg/g), and k_2 is the pseudo second order rate constant for the sorption process (g/mg x h).

A plot of $1/(q_e - q_t)$ versus t should give a straight line with slope of k_2 and an intercept equal to $1/q_e$. This model is not suitable for our adsorbate/adsorbent system because the adsorption is very slow and there is only physisorption between metallosilicate beads and Direct Red 95 dye. Consequentely the correspondence of the experimental data with the proposed pseudo second order model is the least. Figure 11b shows the matching of the experimental data to this model, the calculated k and q_e parameters being included in table 5.

Elovich model

This model has been often used suitably in chemisorption on heterogeneous materials [29, 31] and has been found

Table 4
PARAMETERS CORRESPONDING TO THE ADSORPTION MODELS

Langmuir		Freundlich		Temkin		Dubinin-Radushkevish	
q_m (mg/g)	K_a (L/mg)	K_F (mg/g)	n	K_T (L/g)	b_T (kJ/mol)	Q_m (mg/ g)	B_D (mol^2/J^2))
1.499	0.361	0.21	2.913	4.336	8.131	1.2664	10^{-7}

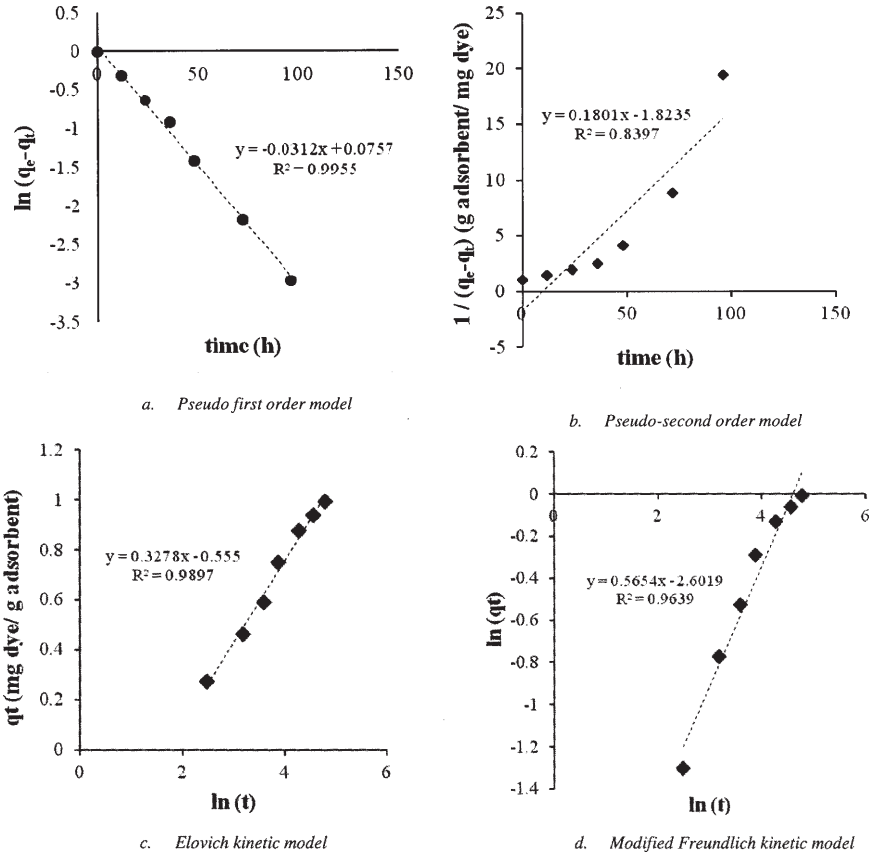

a. *Pseudo first order model*

b. *Pseudo-second order model*

c. *Elovich kinetic model*

d. *Modified Freundlich kinetic model*

Fig. 11. Kinetic models applied to the sorption of direct red dye on metallosilicate beads (Temperature = 298 K, contact time = 120 h, initial dye concentration = 20 mg/L, adsorbent dose 0.15 g/ 10 mL)

Kinetic model	Parameters	R^2
Pseudo first order model	k_1 = 0.0312 (h^{-1})	0.9955
Pseudo-second order model	k_2 = 0.1801 (g/ mg · h)	0.8397
Elovich model	a = 0.0603 (mg dye/g adsorbent)) b = 0.3278 (mg dye/g adsorbent)	0.9897
Modified Freundlich kinetic model	k_f = 0.0037 (L/mg) m = 1.7687	0.9639

Table 5
PARAMETERS OF THE KINETIC MODELS USED TO DESCRIBE THE ADSORPTION OF DIRECT RED 95 DYE BY METALLOSILICATE BEADS

to cover a wide range of slow adsorption processes. The Elovich model is represented by the following equation:

$$q_t = b \ln (a/b) + b \ln (t) \quad (12)$$

where $q_t$is the amount of adsorbed dye at time t, a is the sorption constant of the dye (mg/g) and b is the desorption constant (mg/g).

The constants a and b can be obtained from the slope and intercept of the linear plot of qt versus ln(t). Table 5 shows the kinetic constants obtained with this model.

Modified Freundlich kinetic model

The linear form of the modified Freundlich equation (13) is as follows:

$$\ln q_t = \ln(k_f \cdot C_0) + \left(\frac{1}{m}\right) \cdot \ln t \quad (13)$$

where q_t is the amount of direct dye (mg/g) adsorbed at time t, k_f is the apparent adsorption rate constant [L/(g x min)]; C_0, is the initial dye concentration (mg/L); t, is the contact time (h); m, is the Kuo-Lotse constant.

The values of k and m are used empirically to evaluate the effect of surface loading and ionic strength on the adsorption process.

Figure 11 shows the agreement between the experimental data and the equations of adsorption kinetic models (pseudo first order model, pseudo-second order model, Elcovich model and modified Freundlich model) for the adsorption of direct dye onto metallosilicate beads.

The valuesof regression correlation coefficient (R^2) shown in table 5 indicates that the pseudo first order model fits best with the experimental data, then come the Elovich model and respectively the modified Freundlich kinetic model, while the pseudo-second order model is the least satisfactory.

Conclusions

This work studied the synthesis, characterization and testing of hierarchical metallosilicate beads as adsorbent. The adsorption process was dependent on *p*H value of solution, adsorbent dosage and initial dye concentration. The removal efficiency increased significantly with the increase of the metallosilicate beads loading and reached a value of 74.5% for an initial dye concentration C_0 = 20 mg/L and 15g adsorbent/L. The Langmuir and Dubinin-Radushkevish is otherms gave the best matching with the experimental data. The obtained monolayer saturation capacity (mg dye/g adsorbent) suggests that the affinity of the metallosilicate beads for the direct dye is moderate. Among various kinetic models used to describe the adsorption of Direct Red 95 dye on metallosilicate beads the pseudo first order model (R^2 = 0.9955) provided the best agreement with the recorded values.

References

1.ROBINSON, T., MCMULLAN, G., MARCHANT, R., NIGAM, P., Bioresour Technol., **77**, no. 3, 2001, p. 247.
2.FORGACS, E., CSERHATI, T., OROS, G., Environ. Int., **30**, 2004, p. 953.
3.EL-SHAHATE, M.I.S., EL-SAIED M.A.F., SAYED, H. and EL-RAHMAN, A.M., Journal of Materials Science and Engineering B, 2011, p. 97.
4.ALVER, E., METIN, A.Ü., Chem. Eng. J., **200–202**, 2012, p. 59.
5.ANBIA, M., AND SALEHI, S., Dyes Pigm., **94**, nr. 1, 2012, p. 1.
6.CRINI, G., GIMBERT, F., ROBERT, C., MARTEL, B., ADAM, O., MORIN-CRINI, N., DE GIORGI ., BADOT, P.M. , J. Hazard Mater., **153**, no. 1-2, 2008, p. 96.
7.RADITOIU, A., AMARIUTEI, V., RADITOIU, V., WAGNER, L.E., GABOR, R.A., GHIUREA, M., SPATARU, C.I., Mat. Plast., **51**, no. 2, 2014, p. 130.
8.RADITOIU, A., RADITOIU, V., AMARIUTEI, V., NICOLAE, C.A., GABOR, A.R., FRONE, A.N., FIERASCU, R.C., GHIUREA, M., WAGNER, L.E., HUBCA, G., Mat. Plast., **50**, no. 4, 2013, p. 241.
9.ERRAIS, E., DUPLAY, J., ELHABIRI, M., KHODJA, M., OCAMPO, R., BALTENWECK-GUYOT, R., DARRAGI, F., Colloid Surf. A , **403**, 2012, p. 69.
10.AL-RASHED, S.M. AL-GAID, A.A., J. Saudi Chem. Soc., **16**, no. 2, 2012, p. 209.
11.BACCAR, R., BLÁNQUEZ, P., BOUZID, J., FEKI, M., SARR , M., Chem. Eng. J., **165**, 2010, p. 457.
12.BAE, J.H., SONG, D.I., JEON, Y.W., Sep. Sci. Technol., **35**, no. 3, 2000, p. 353.
13.CHUNG-KUNG, L., SHIN-SHOU, L., LAIN-CHUEN, J., CHENG-CAI, W., KUEN-SONG, L., MENG-DU, L., J. Hazard Mater, **147**, 2007, p. 997.
14.NWABANNE, J.T., MORDI, M.I., African .J.Bio Tech., **8**, 2009, p. 1555.
15.DURAL, M.U., CAVAS, L., PAPAGEORGIOU, S.K., KATSAROS, F.K., Chem. Eng. J., **168**, no. 1, 2011, p.77.
16.KHOKHLOVA, T.D., NIKITIN, Y.S., DETISTOVA, A.L., Adsorpt. Sci. Technol., **15**, no. 5, 1997, p. 333.
17.KARADAG, D., TURAN, M., AKGUL, E., TOK, S., FAKI, A., *J. Chem. Eng. Data*, **52**, 2007, p. 1615.
18.CHANDRA, T.C., MIRNA, M., SUDARYANTO, Y., ISMADJI, S., Chem Eng J., **127**, no. 1-3, 2007, p.121.
19.SHAOBIN, W., HUITING, L., LONGYA, X., J. Colloid Interface Sci., **295**, 2006, p. 71.
20.HO, K.Y., MCKAY, G.,. YEUNG, K.L, Langmuir, **19**, 2003, p. 3019.
21.KUMAR, P.S., RAMALINGAM, S., SATHISHKUMAR, K., Korean J. Chem. Eng., **28**, no. 1, 2011, p. 149.
22.WAWRZKIEWICZ, M., Chem. Eng. J., **217**, 2013, p. 414.
23.ABOU-MESALAM, M. M,. Adsorption, **10**, 2004, p. 87.
24.E. VOUDRIAS, F. FYTIANOS AND E. BOZANI, Global Nest, The Int. J., **4**, 2002, p. 75.
25.XIONGA, C., LIA, Y., WANGA, G., FANGB. L., ZHOUA, S., YAOA, C.,CHENA, Q. ZHENGC, X., QID, D., FUD, Y., ZHUD, Y., Chem. Eng. J., **259**, 2015, p. 257.
26.MUNTEAN, S.G., SIMU, G., SFARLOAGA, P., BOLOGA, C., Rev. Chim. (Bucharest), **61**, no. 1, 2010, p. 70.
27.BECK, J.S., VARTULI, C., ROTH, W.J.,. LEONOWICZ, M.E, KRESGE, C.T., SCMMITT, K.D., CHU, C.T-W., OLSON, D.H., SHEPPARD, E.W., MCCULLEN, S.B., HIGGINS, J.B., SCHLENKER, J.L., J. Am. Chem. Soc., **114**, 1992, p. 10834.
28.NISTOR, A., STIUBIANU, G., RACLES, C., CAZACU, M., Mate. Plast., **48**, no. 1, 2011, p. 33.
29.MAMALIGA, I., Mat. Plast., **41**, no. 4, 2004, p. 264.
30.MIKHAIL, R.S., BRUNAUER, S., BODOR, E.E., J. Colloid Interface Sci., **26**, 1968, p. 45.
31.HAGYMASSY JR, J., BRUNAUER, S., MIKHAIL, R.S., J. Colloid Interface Sci., **29**, 1969, p. 485

Manuscript received: 12. 01.2015